

Type I ELM Energy and Particle Losses in JET H-modes and implications for ITER

A. Loarte 1) and JET EFDA Contributors*

1) European Fusion Development Agreement, Close Support Unit Garching, Max-Planck-Institut für Plasmaphysik, D-85748 Garching bei München, Germany

* See Annex in IAEA 2002 J. Pamela OV-1/1.4

e-mail contact of main author : Alberto.Loarte@efda.org

Abstract. Measurements during Type I ELMs in JET show that the value of the bulk plasma ELM energy loss is determined by the pedestal plasma parameters during the ELM. For fixed global plasma parameters (I_p , B_t , δ) the ELM energy drop decreases with increasing pedestal plasma density. This is due to a reduction of the ELM conductive losses (due to the change of edge temperature at the ELM), while convective losses (due to the change of edge density at the ELM), remain approximately constant. Empirical correlations of the Type I ELM energy losses with pedestal plasma collisionality and ion transport time in the SOL are described, together with the implications of these findings for ITER. Physics mechanisms that may lead to the observed experimental correlations are discussed.

1. Introduction

JET has achieved plasma discharges that meet the ITER requirements, in terms of q_{95} , Z_{eff} and normalised parameters. In particular, plasmas with simultaneous $\langle n_e \rangle / n_{\text{GW}} = 100\%$ ($n_{\text{GW}} = \text{Greenwald density}$), $H_{98} \sim 1$ ($H_{98} = \text{energy confinement time normalised to ITER H98}(y,2)$ scaling), $P_{\text{INP}} / P_{\text{L-H}} \sim 1.4$ ($P_{\text{L-H}} = \text{threshold power for L-H transition normalised to the ITER-96 scaling}$) and $\beta_N \sim 2$ have been reproducibly obtained in JET by operating in Type I ELMy H-modes at high triangularities [1, 2]. One of the main problems that remains for the full extrapolability of these discharges to ITER is the transient energy loads onto the divertor target associated with the Type I ELMs. These loads are of no concern in present experiments but, when extrapolated to ITER, the ELM energy loads may lead to a severe limitation of the divertor target lifetime due to enhanced erosion, caused by sublimation (for a carbon target) or melting (for a tungsten target) [3]. In determining the ELM energy and particle loads to the divertor two aspects have to be studied : the ELM-induced losses of energy and particles from the bulk plasma and the corresponding fluxes which reach the divertor target. The first aspect is the subject of this paper, while the second one is discussed in a companion paper [4].

2. Change of Bulk Plasma Parameters during JET Type I ELMs

The changes of bulk plasma parameters due to Type I ELMs in JET are determined by fast electron temperature with ECE and line integrated measurements of the electron density and the plasma soft X-ray bremsstrahlung emission. Type I ELMs cause a sudden decrease of the plasma parameters (n_e and T_e) in a time scale of $\sim 200 \mu\text{s}$ during which an enhanced MHD activity is observed in the Mirnov coils [5]. The collapse of the electron temperature during Type I ELMs in JET occurs typically over the outer 15-25 % of the plasma radius as shown in Fig. 1. The width of this ‘‘ELM affected’’ region decreases with increasing plasma triangularity and decreases slightly with increasing fuelling rate (edge density). Both of these trends are in qualitative agreement with predictions of the radial width of the most unstable mode in the ballooning-peeling ELM model [6]. The duration of the ELM collapse ($\tau_{\text{ELM-MHD}}$) has been determined in JET by analysis of the Mirnov coil signals during ELMs and by determining the duration of the collapse phase of the pedestal plasma parameters from the soft X-ray edge chords emission. In JET, $\tau_{\text{ELM-MHD}}$ is in the range $(225 \pm 75) \mu\text{s}$ for a large range of discharge parameters [5], as seen in Fig. 2. It is particularly interesting to note that for fixed magnetic field (2.7T, where most measurements are available), $\tau_{\text{ELM-MHD}}$ is weakly dependent on the pedestal plasma temperature (T_{ped}) and density (n_{ped}) in contrast with what is expected

from a Kadomstev-type estimate of the reconnection time ($\sim n_{\text{ped}}^{1/4} T_{\text{ped}}^{3/4}$). MHD models of the ELM MHD collapse, similar to those developed to understand β collapses in ITB discharges [7] or sawtooth reconnection [8], will have to be developed in order to understand the physical processes that determine this time scale and its extrapolation to ITER.

The collapse of the pedestal density and temperature caused by the ELM is correlated with their values before the ELM collapse. Increasing n_{ped} decreases the relative drop of the pedestal temperature but not of the density, as shown in Fig. 3. As a consequence, ELM conductive losses (due to the change of edge temperature at the ELM) $\Delta W_{\text{ELM}}^{\text{cond}}$, decrease with increasing n_{ped} , while convective losses (due to the change of edge density at the ELM) $\Delta W_{\text{ELM}}^{\text{conv}}$, remain approximately constant, similar to findings in other experiments [9]. For some magnetic configurations, at sufficiently high density, the Type I ELMs cause no collapse of the electron temperature, as shown in Fig. 3. In these Type I ELMs (named “Minimum” Type I ELMs) the loss of plasma energy during an ELM, ΔW_{ELM} ($\Delta W_{\text{ELM}} = \Delta W_{\text{ELM}}^{\text{conv}} + \Delta W_{\text{ELM}}^{\text{cond}}$), is due completely to the loss of particles associated with the ELM and, hence, the ELM energy loss from the bulk plasma is purely convective [10]. For these ELMs the normalised (to the pedestal energy $W_{\text{ped}} = 3 n_{\text{e,ped}} T_{\text{e,ped}} V_{\text{plasma}}$, $T_{\text{i,ped}} \sim T_{\text{e,ped}}$) energy drop $\Delta W_{\text{ELM}}/W_{\text{ped}}$ is 5 %, which is well within the acceptable range from ITER divertor target lifetime considerations [11].

3. Type I ELM Energy and Particle Losses in JET Experiments

Previous JET experimental evidence had suggested a strong link between ELM size and frequency, which is usually observed in ELMy H-mode experiments with gas fuelling [12]. The reduction of the ELM energy losses with higher pedestal densities obtained at larger puffing rates was, hence, linked invariably to higher ELM frequencies. Experiments at JET in discharges with high triangularities ($\delta > 0.4$) [1] or with high levels of additional heating ($P_{\text{INP}}/P_{\text{L-H}} > 2.5$) [13] have shown that this link can be broken. In these conditions, a decrease of the ELM frequency and a decrease of $\Delta W_{\text{ELM}}/W_{\text{ped}}$ are simultaneously obtained with increasing pedestal density and gas fuelling level [1, 2, 10, 13]. This new experimental evidence has demonstrated that the ELM energy loss in JET is determined by the plasma parameters before the ELM (n_{ped} , T_{ped}), while the ELM frequency is a result of the ELM size and the inter-ELM energy transport. Examination of JET discharges over a large range of plasma parameters has shown that the normalised ELM loss ($\Delta W_{\text{ELM}}/W_{\text{ped}}$) is well correlated with the value of the pedestal collisionality (ν_{ped}^*) before the ELM, as shown in Fig. 4. In this figure, the range of allowed ELM energy loss for the ITER reference inductive scenario is shown together with the expected ITER collisionality. The upper allowed levels marked by arrows come from estimates [11], which expand a range of modelling hypotheses (based on experimental results [14]), alternative ITER divertor designs and various assumptions on the percentage of ELM energy reaching the divertor. Based on this empirical scaling and if all of the energy lost from the bulk plasma would reach the ITER divertor target, Type I ELMs energy losses would impose a severe limitation on the divertor target lifetime. The empirical scaling found for JET is $\Delta W_{\text{ELM}}/W_{\text{ped}} = 0.076 [\nu_{\text{ped}}^*(\text{neo})]^{-0.31}$, where $\nu_{\text{ped}}^*(\text{neo})$ is the neoclassical electron collisionality calculated with the values of the plasma parameters at the top of the pedestal before the ELM crash. On the contrary, ELM particle loss and, hence, ELM convective energy losses are very weakly dependent on pedestal plasma parameters and their value is estimated to be $\Delta W_{\text{ELM}}^{\text{conv}}/W_{\text{ped}} \sim (5 - 8) \%$ for JET. This value and behaviour of the ELM convective losses with pedestal plasma parameters is in agreement with measurements in DIII-D [9]. Removing this constant convective ELM energy loss contribution (assumed $\sim 5\%$) from the data in Fig. 4 leads to a scaling for the conductive

ELM energy loss in JET as $\Delta W_{\text{ELM}}^{\text{cond}}/W_{\text{ped}} = 0.032 [v_{\text{ped}}^*(\text{neo})]^{-0.51}$, which has a somewhat stronger dependence on v_{ped}^* than the total ELM energy loss.

Although the detailed description of the ELM energy flux to the divertor is the subject of a separate paper [4], we present here the experimental evidence for the existence of a high energy electron flux during the ELM collapse which occurs in a different time scale of the main ion flux caused by the ELM, as shown in Fig. 5. This figure shows the collapse of the pedestal plasma temperature in the phase of ELM enhanced MHD activity. During this MHD phase an increased signal in the soft x-ray chord that intersects the inner divertor target is measured. This increased soft x-ray emission is due to the bremsstrahlung emission from electrons with energies \sim keV (or larger) as they slow down into the divertor target material [15]. As shown in Fig. 5, the increase of the inner divertor ion flux (as measured by the D_α emission) associated with the ELM occurs $\sim 200 \mu\text{s}$ later than the increase of soft X-ray emission, which marks the arrival of the hot electrons. This delay is compatible with typical parallel transport time scales for pedestal ions to reach the inner divertor from the outer midplane. The observation of a different ELM electron and ion flux temporal behaviour is consistent with the formation of a high energy sheath that restricts the energy flux from the pedestal plasma, that connects to the divertor target, during the ELM-MHD phase in which the ion flux is low, as proposed in [3]. Following this hypothesis, the characteristic time for the ELM energy flux is determined by the ion parallel transport. Measurements of Type I ELM energy flux show a good correlation with this hypothesis [16], which is also consistent with the loss of plasma current observed during the ELM [17]. Furthermore, the ELM energy loss would be determined by the competition between the impedance of the sheath to the flux of energy (determined by the ion parallel transport time) and the period with enhanced ELM MHD activity ($\tau_{\text{ELM-MHD}}$). $\tau_{\text{ELM-MHD}}$ in JET is weakly dependent on plasma parameters, hence, following the hypothesis in [3], an inverse correlation of $\Delta W_{\text{ELM}}/W_{\text{ped}}$ with $\tau_{\parallel}^{\text{Front}}$ (SOL ion transit time calculated with pedestal plasma parameters) is expected. This correlation has been confirmed for JET discharges over a wide range of plasma parameters, as shown in Fig. 6. If the sheath impedance mechanism solely determines the ELM energy loss, the ELM losses expected in ITER would be compatible with an acceptable divertor target lifetime.

4. Discussion and Conclusions

Our present understanding of the ELM energy and particle losses is still based mostly on empirical scalings, which are providing the basis for the development of physics models. No model for the ELM losses developed so far provides quantitative estimates that can be compared with the experiment. However, the different behaviour of the ELM particle and energy losses with increasing v_{ped}^* (or n_{ped}) can be used to shed some light on which are the likely physical processes involved in the Type I ELM energy and particle losses. In first place, it is obvious that increasing v_{ped}^* decreases the value of the pedestal bootstrap current, which changes pedestal MHD plasma stability [6]. This may indeed affect the radial structure of the most unstable MHD modes but, on its own, pure MHD estimates cannot provide an explanation for the varying contributions with v_{ped}^* of convection and conduction in the observed ELM energy losses. On the other hand, a purely sheath limited ELM energy loss mechanism would lead to a similar decrease of the ELM energy and particle losses with $\tau_{\parallel}^{\text{Front}}$, as the energy and ion losses are linked through the electric field established in the sheath. Although there is a clear decrease of $\Delta W_{\text{ELM}}/W_{\text{ped}}$ with $\tau_{\parallel}^{\text{Front}}$, the experiment shows that $\Delta W_{\text{ELM}}^{\text{conv}}/W_{\text{ped}}$ and $\Delta N_{\text{ELM}}/N_{\text{ped}}$ (normalised particle losses to the pedestal particle content) are independent of $\tau_{\parallel}^{\text{Front}}$. This is in contradiction with a purely sheath limited mechanism determining the ELM losses. A possible explanation for the observed v_{ped}^* dependence of $\Delta W_{\text{ELM}}/W_{\text{ped}}$ and $\Delta W_{\text{ELM}}^{\text{cond}}/W_{\text{ped}}$ comes from considerations of energy and

particle transport in the ergodised edge during the ELM, which is presently under theoretical study [18]. In the ELM ergodised layer, the electron conductive losses can be described by the Rechester-Rosenbluth model [19], hence, $\Delta W_{\text{ELM}}^{\text{cond}} \sim \tau_{\text{ELM-MHD}} \times D_{\text{RR}} \times T_{\text{ped}}^{7/2}/L_c$, where D_{RR} is the Rechester-Rosenbluth field line diffusion coefficient and L_c is the correlation length of the ergodised field. Convective losses are more difficult to estimate quantitatively in this model and are the subject of further studies. In this physical picture, the normalised ELM conductive losses scale as $\Delta W_{\text{ELM}}^{\text{cond}}/W_{\text{ped}} \sim (T_{\text{ped}}^{1/2}/v_{\text{ped}}^*)$, assuming that D_{RR} is independent of n_{ped} , T_{ped} and $L_c \sim \pi R q_{95}$. This scaling resembles the experimental one but the collisionality dependence is stronger than that seen in experiment, where $\Delta W_{\text{ELM}}^{\text{cond}}/W_{\text{ped}} \sim [v_{\text{ped}}^*(\text{neo})]^{-0.51}$. A possible explanation for this discrepancy comes from the sheath impedance to heat flux that can provide the mechanism for the limitation of the heat flux at low collisionalities, which electron conduction cannot on its own, and that is not included in this model.

From the above discussion, it is clear that we have not yet developed a model for the ELM energy loss that allows a fully physics-based extrapolation of present JET results to ITER. Despite this, empirical trends of the Type I ELM energy and particle losses have been identified and their validity tested over a large range of plasma parameters in JET, improving greatly our confidence in the extrapolation of present results to ITER. On the basis of these empirical trends, the expected ELM energy fluxes on the ITER divertor are close to being marginal for an acceptable divertor target lifetime [11]. JET is the only device that can achieve pedestal plasma parameters with similar temperatures and collisionalities to those expected in ITER. Therefore, the development and validation of theoretical or semi-empirical models for ELM energy losses, which can be used with confidence to extrapolate experimental results to ITER, is most relevant under the JET experimental conditions.

5. Acknowledgements

The main author would like to acknowledge direct contributions of the following contributors to the EFDA-JET workprogramme : M. Becoulet, G. Saibene, R. Sartori, D.J. Campbell, T. Eich, A. Herrmann, W. Suttrop, B. Alper, G. Matthews, J. Ongena and P. Innocente. Contributions from K. Lackner, Y. Igitchanov and G. Federici on energy transport in ergodised layers, MHD reconnection physics and effects of ELM energy fluxes on the ITER divertor target are gratefully acknowledged.

6. References

- [1] SAIBENE, G. et., al., Plasma Phys. Control. Fusion **44** (2002) 1769.
- [2] ONGENA, J., et al., paper IAEA-CN94/EX/C2-4, this Conference.
- [3] JANESCHITZ, G., et al., J. Nucl. Mat. **290-293** (2001) 1.
- [4] MATTHEWS, G.F., et al., paper IAEA-CN94/EX/D1-1, this Conference.
- [5] BECOULET, M., at al., IAEA Tech. Comm. Divertor Concepts, France, 2001.
- [6] PARAIL, V., et al., paper IAEA-CN94/TH/P3-08, this Conference.
- [7] CALLEN, J.D., et al., Phys. Plasmas **6** (1999) 2963.
- [8] WESSON, J.A., Plasma Phys. and Control. Fus. Res., Vol. 2, p. 79, IAEA, Vienna, 1991.
- [9] LEONARD, A., et al., Plasma Phys. Control. Fusion **44** (2002) 945.
- [10] LOARTE, A., et., al., Plasma Phys. Control. Fusion **44** (2002) 1815.
- [11] FEDERICI, G., et al., 15th PSI Conference, Japan, 2002. To be published in J. Nuc. Mat.
- [12] FISHPOOL, G., Nucl. Fusion **38** (1998) 1373.
- [13] SARTORI, R., et al., Plasma Phys. Control. Fusion **44** (2002) 1801.
- [14] LOARTE, A., et al., 15th PSI Conference, Japan, 2002. To be published in J. Nuc. Mat.
- [15] GILL, R., et al., et al., Nucl. Fusion **38** (1998) 1461.
- [16] EICH, T., et al., 15th PSI Conference, Japan, 2002. To be published in J. Nuc. Mat.
- [17] SOLANO, E., et al., IEA ELM Workshop, UK, 2002.
- [18] BECOULET, M., et al., 2002, to be published.
- [19] RECHESTER, A., et al., Phys. Rev. Lett. **40** (1978) 38.

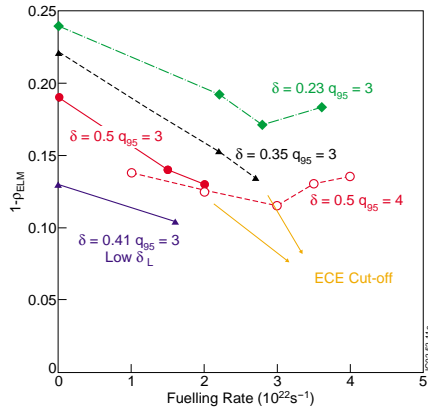


Figure 1. Normalized radial extent ($= r/a$) of the ELM affected zone for the electron temperature profile in JET discharges in various magnetic configurations versus fuelling rate.

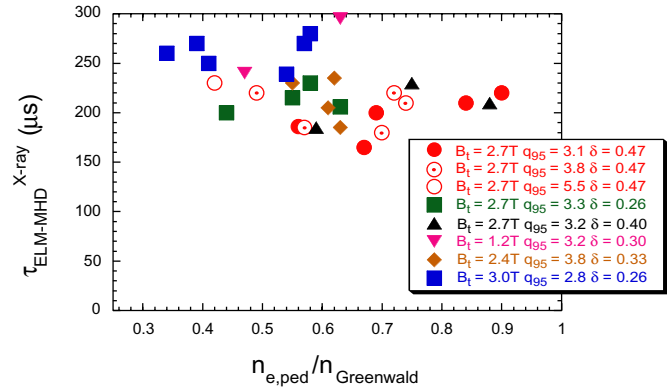


Figure 2. Time duration of the edge plasma collapse measured by soft X-ray emission for a large range of JET ELMy H-mode plasmas.

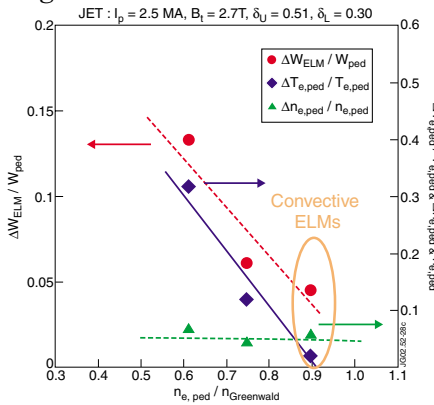


Figure 3. Normalized ELM energy loss ($\Delta W_{ELM} / W_{ped}$), pedestal temperature ($\Delta T_{e,ped} / T_{e,ped}$) and density ($\Delta n_{e,ped} / n_{e,ped}$) drop versus pedestal density normalised to the Greenwald limit for JET discharges.

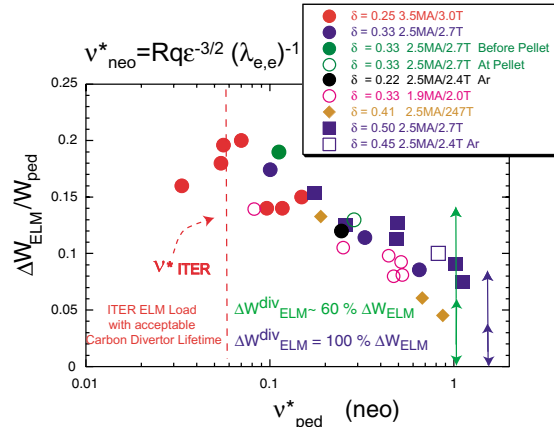


Figure 4. Normalised Type I ELM energy loss ($\Delta W_{ELM} / W_{ped}$) versus pedestal plasma collisionality for a large range of JET ELMy H-mode plasmas. Estimates for the range of acceptable ELM energy loss in ITER are shown by arrows.

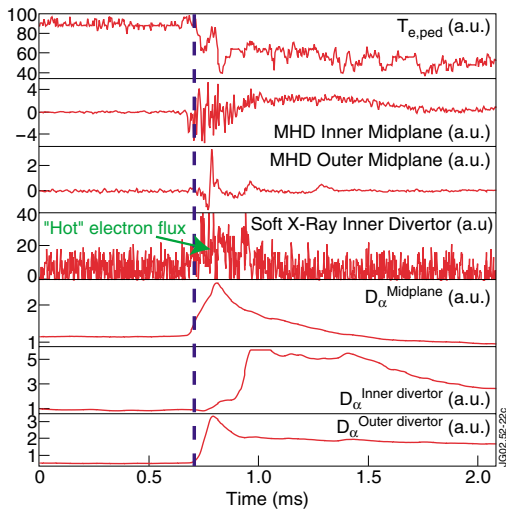


Figure 5. Measurements of the ELM pedestal temperature collapse $T_{e,ped}$, inner divertor soft x-ray emission and D_{α} emission at various locations (midplane, inner and outer divertor).

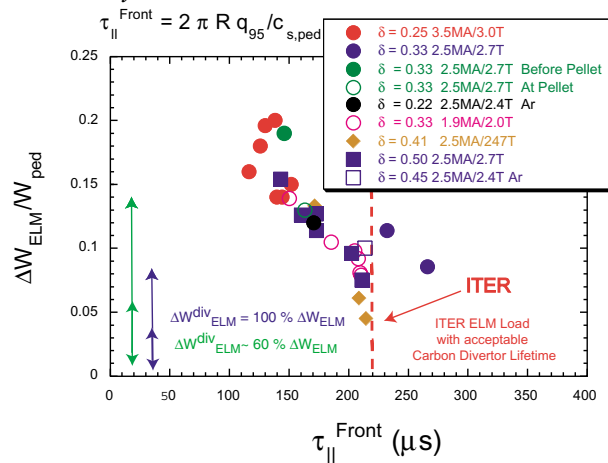


Figure 6. Normalised Type I ELM energy loss ($\Delta W_{ELM} / W_{ped}$) for JET ELMy H-modes versus SOL ion flow parallel time calculated for the pedestal plasma parameters ($\tau_{||}^{Front}$) for a large range of JET ELMy H-mode plasmas. Estimates for the range of acceptable ELM energy loss in ITER are shown by arrows.